

Slip Effects on Heat and Mass Transfer in MHD Power-Law Fluid Flow



By

Saba Javaid

Supervised by

Dr. Asim Aziz

DEPARTMENT OF MATHEMATICS

SCHOOL OF NATURAL SCIENCES

NATIONAL UNIVERSITY OF SCIENCES AND TECHNOLOGY

ISLAMABAD

2015

Slip Effects on Heat and Mass Transfer in MHD Power-Law Fluid Flow

By
SABA JAVAID

A thesis submitted in partial fulfillment of the requirement for the degree of
Masters of Philosophy in Mathematics

Supervised By:
Dr. ASIM AZIZ

DEPARTMENT OF MATHEMATICS
SCHOOL OF NATURAL SCIENCES
NATIONAL UNIVERSITY OF SCIENCES AND TECHNOLOGY,
ISLAMABAD

2015

National University of Sciences & Technology**M.Phil THESIS WORK**

We hereby recommend that the dissertation prepared under our supervision by: SABA JAVAID, Regn No. NUST201361951MSNS78013F Titled: Slip Effects on Heat and Mass Transfer of MHD Power-Law Fluid be accepted in partial fulfillment of the requirements for the award of **M.Phil** degree.

Examination Committee Members1. Name: Dr. Moniba ShamsSignature: 2. Name: Dr. Mazhar IqbalSignature: 3. Name: Dr. Noreen Sher AkbarSignature: 4. Name: Dr. Sohail NadeemSignature: Supervisor's Name: Dr. Asim AzizSignature: 

Head of Department

08-09-2015

Date

COUNTERSIGNEDDate: 8/9/15

Dean/Principal

Declaration

I certify that this research work titled “Slip Effects on Heat and Mass Transfer in MHD Power-Law Fluid Flow” is my own work. The work has not been presented elsewhere for assessment. The material that has been used from other sources it has been properly acknowledged / referred.

Signature of Student

SABA JAVAID

**Slip Effects on Heat and Mass Transfer in
MHD Power-Law Fluid Flow**

Saba Javaid

*I dedicate this modest effort to my honorable
and respected parents Muhammad Yousaf Javaid (Late) and Shaista
Javaid,
who are always a home of encouragement for me.*

Acknowledgements

Allah Almighty is the only who is most gracious and compassionate and admirable of all the admirations and praises. I am greatly obliged to my Almighty Allah, for His continuous direction, provision, assistance and love in each and every aspect of life. He is the one and only who consecrated me with chance to acquire and communicate with the very knowledge to do effort in this ground or field. It is merely the consecration of the All-knowing being to give upon us His Holy Prophet (Sallallahu Alaihay Wa'alihi wasalam) the last human appearance of his complete information, who has deposited all ground of knowledge and will continue the source of all intelligence that is to inspire in the forthcoming.

Here, I would like to acknowledge NUST to providing me such a favourable environment to conduct this research. I would also like to offer my sincere gratitude to my supervisor Dr. Asim Aziz for his excellent supervision merged with his affection and obligation, without him I would have not been able to commence this current research study.

My heartiest and sincere salutations to my parents, who put their greater efforts in making me a good human being. I also feel grateful to my dearest brother Muhammad Hamza Javaid and my sister Sahar Javaid, who never let me down and always fortified me throughout the hard period of my research work. I also acknowledge my dear friends Tayyaba, Wajeeha, Aneela, and Javeria from the core of my heart for their help, sustenance and effort at lifting me up whenever I was doleful.

Saba Javaid

Abstract

In this dissertation, the problem of boundary layer flow and heat transfer of MHD power-law fluid over a porous sheet in the presence of partial slip is investigated numerically. We assume a temperature dependent thermal conductivity and slip conditions are employed in terms of the shear stress. The suitable similarity transformations are used, to transform the governing partial differential equations (PDEs) into a system of nonlinear ordinary differential equations (ODEs). The resulting system of ODEs is solved numerically using Matlab bvp4c solver. The numerical values obtained for the velocity and temperature depend on power-law index, slip parameters, permeability, suction/injection parameter, thermal conductivity parameter, radiation parameter, Prandlt number, Nusselt number, Schmidt number and Soret number. The effects of various parameters on the flow and heat transfer characteristics are presented through graphs and tables and discussed from physical point of view.

Table of Contents

1	Introduction	1
2	Preliminaries	6
2.1	Fluid and Flow	6
2.2	Steady and Unsteady Flows	7
2.3	Laminar and Turbulent Flow	7
2.4	Compressible and Incompressible Flow	7
2.5	Viscosity	8
2.6	Newtonian and non-Newtonian fluid	8
2.6.1	Power-Law Model	9
2.7	Generalized Continuity Equation	9
2.8	The Momentum Equation	10
2.8.1	Magnetohydrodynamics	10
2.8.2	Porosity	11
2.9	Heat Transfer	12
2.9.1	Conduction	12
2.9.2	Convection	13

2.9.3	Radiation	14
2.10	Energy Equation	14
2.11	Mass Transfer	15
2.11.1	Concentration Equation	15
3	Slip effects on flow and heat transfer of MHD power-law fluid by a porous sheet with variable thermal conductivity and thermal radiation	16
3.1	Introduction	16
3.2	Mathematical Modeling	17
3.3	Method of Solution	19
3.4	Results and Discussion	23
4	Slip effects on flow, heat and mass transfer of MHD power-law fluid by a porous sheet with variable thermal conductivity and thermal radiation	35
4.1	Introduction	35
4.2	Mathematical Modeling	36
4.3	Method of Solution	36
4.4	Results and Discussion	38
5	Conclusion	44
	References	46

Chapter 1

Introduction

The layer of fluid that flows adjacent to its bounding surface is called the boundary layer. The boundary layer flow plays vital role in many aspects of fluid mechanics and has been studied extensively. The applications of boundary layer theory include; the calculation of friction drag of a flat plate a ship, an airfoil, the body of an airplane or a turbine blade cooling devices and food processing industry etc. Prandtl [1] first presented the concept of boundary layer to identify the flow behavior of fluid near a solid boundary. Blasius [2] solved the well-known boundary layer equation for a moving flat plate problem and obtained a power series solution of the model. In the theory of non-newtonian fluid this concept was introduced by Pascal [3]. A comprehensive literature survey on boundary layer theory and associated topics can be found in the studies of [4–7].

In recent years, boundary layer models include the analysis of heat transfer, because these type of procedures exist in nature and have industrial applications like heat exchanger, recovery of petroleum resources, fault zones, catalytic reactors, cooling devices, chemical reactions in a reactor chamber comprising of rectangular ducts, deposition of

chemical vapor on surfaces etc. A detailed literature on forced/natural convection of viscous fluids past their bounding surface can be found in the books of [8–10]. Kumari et. al [11] investigated the non-Darcian effects on forced convection heat transfer over a flat plate in a highly porous medium. A computational analysis of heat transfer in case of forced convection fluid flow on a heated flat plate embedded in a porous medium is performed by Luna and Mndez [12]. Khaled and Vafai [13] deliberated the various flow models in porous medium with applications in biological areas such as diffusion in brain tissues, tissue generation process, blood flow in tumors, bio-heat transfer in tissues and bio-convection. The interaction of free convection with thermal radiation of a fluid along with moving plate was studied by Makinde [14]. In [15], Ibrahim et. al examined the unsteady MHD, mixed convection micropolar fluids with viscous dissipation and radiation. Recently, the effect of variable thermal conductivity on a flow of power-law fluids over stretching sheet with heat transfer has been studied by [16].

There are number of studies available in which partial slip boundary conditions have been employed to make the problems physically well-posed. In [17–19] authors employed slip boundary conditions on a boundary layer forced convective flow with heat and mass transfer of an incompressible fluid past a porous plate embedded in a porous medium. Pal and Talukdar [20] studied an unsteady magnetohydrodynamic convective heat and mass transfer past a vertical permeable plate using slip boundary conditions with thermal radiation and chemical reaction. Recently, Khan et. al [21] examined the flow and heat transfer of carbon nanotubes (CNTs) subjected to Navier slip and uniform heat flux boundary conditions. There are many models proposed for non-Newtonian fluids. The theory of boundary layer for every model is also available in the literature. It is away

from this work to revisit the vast amount of literature on the boundary layers of different non-Newtonian fluid models. A limited work can be referred as examples on the topic in [22–28]. The efforts have been directed towards understanding the friction and heat transfer characteristics of non-Newtonian fluids. The power-law viscosity model of non-Newtonian fluid is one in which the shear stress varies according to a power function of the strain rate. A good representation found for pseudo-plastic behavior of fluid is power-law model. . Acrivos et al. [29] studied the boundary layer flow of power-law fluid past a horizontal flat plate including heat transfer. Schowalter [30] formulated the two and three dimensional boundary layer equations and found some new solutions for the equations. Lee and Ames [31] found the similarity solutions for power-law fluid which is the extension of the above work. Andersson et al. [32] examined the electrically conducting power-law fluid in the presence of transverse magnetic field in the boundary layer flow. The problem of MHD flow and heat transfer of an electrically conducting, non-Newtonian power-law fluid past a stretching sheet in the presence of transverse magnetic field was studied by Chein [33]. Seddeek [34] presented an analysis to study the effect of suction and injection on heat transfer for power-law non-Newtonian fluid. The flow in a boundary layer includes the effects of radiation and a cooled surface temperature.

In a moving fluid when heat and mass transfer occur simultaneously the relations between the fluxes and the driving potentials are of more complex nature. It has been found that an energy flux can be generated not only by temperature gradients but by composition gradients as well. Recent additions considering power-law fluid with heat and mass transfer in various physical situations are given by [35, 36].

In all the above studies the thermophysical properties of the ambient fluid were as-

sumed to be constant with constant thermal conductivity. However many processes in engineering occur at high temperature and it is fully understood that these properties may change with temperature. Moreover, a knowledge on radiation heat transfer becomes very important for design of reliable equipment, nuclear plants, gas turbines and various propulsion devices or aircraft, missiles, satellites and space vehicles. On the basis of these applications, radiation effect on flow and heat transfer problems with variable thermo-physical properties has become important industrially. Several publications are available on the effect of radiation on flow and heat transfer flow (see, for example, [37–45]).

In this thesis we extended the work of Bhattacharya [18] to investigate the slip effects on the heat and mass transfer of MHD boundary layer flow of power-law fluid over a permeable plate embedded in a uniform porous medium with variable thermal conductivity and thermal radiation. The resulting governing equations are transformed into a system of non-linear ordinary differential equations by applying a suitable similarity transformation. These equations are then solved numerically using Matlab bvp4c code. The numerical results are discussed for various physical parameters effecting the flow, heat and mass transfer.

The thesis is arranged as follows: In chapter 2 we present some basic definitions of fluid flow, power-law model of non-Newtonian fluid, magnetohydrodynamics, heat transfer and mass transfer. These basic concepts are used further on describing the flow, heat and mass transfer of power-law fluid. In chapter 3 we discuss the slip effects on flow and heat transfer of electrically conducting power-law fluid over a porous plate embedded in a porous medium with variable thermal conductivity and thermal radiation. The governing equations are solved numerically and results are presented in the form of

graphs and tables. Chapter 4 discusses both heat and mass transfer of MHD power-law fluid under slip conditions. In chapter 3 and 4 the main findings of the investigation are presented. Conclusion to the present work and some suggestions for the future work are given in chapter 5.

Chapter 2

Preliminaries

In this chapter an introduction to the basic ideas of fluid flow, types of fluid flows and governing equations for the fluid flow are stated. In addition an introduction to heat transfer, modes of heat transfer and mass transfer is also presented.

2.1 Fluid and Flow

The substance that continuously alter when a shear stress of any magnitude acts on it, is called a fluid. Fluids are the phases of matter and include liquids, gases, plasmas and to some extent plastic solids. If fluid constantly deforms under the action of any force the phenomenon is called fluid flow.

2.2 Steady and Unsteady Flows

A flow in which the fluid property at a specific point does not change with time is called steady flow i.e.,

$$\frac{\partial \lambda}{\partial t} = 0, \quad (2.1)$$

where λ is any fluid property and $\frac{\partial}{\partial t}$ is the partial derivative with respect to time t . A flow in which fluid property changes with time is called unsteady flow i.e.,

$$\frac{\partial \lambda}{\partial t} \neq 0. \quad (2.2)$$

2.3 Laminar and Turbulent Flow

The flow in which the particles of the fluid move in parallel layers is called laminar flow. In such flow, the path lines of fluid particles do not intersect each other. The flow in which significant mixing take place into fluid particles i.e. fluid particle change directions continuously is called turbulent flow.

2.4 Compressible and Incompressible Flow

The flow type in which the density is constant within the fluid is called incompressible flow. The mathematical equation for the incompressible flow is given by

$$\frac{D\rho}{Dt} = 0, \quad (2.3)$$

where ρ is the density of the fluid and $\frac{D}{Dt}$ is the material derivative given by

$$\frac{D}{Dt} = \frac{\partial}{\partial t} + \mathbf{V} \cdot \nabla. \quad (2.4)$$

In Eq. (2.4) \mathbf{V} represents the velocity of the flow and ∇ is the differential operator. In Cartesian coordinate system ∇ is given as

$$\nabla = \frac{\partial}{\partial x} \hat{i} + \frac{\partial}{\partial y} \hat{j} + \frac{\partial}{\partial z} \hat{k}. \quad (2.5)$$

In Eq. (2.5) $(\hat{i}, \hat{j}, \hat{k})$ are the unit vectors in their respective directions. The fluid flow in which the density variation is not negligible are termed as compressible flow [46].

2.5 Viscosity

Viscosity is a measure of reluctance of fluid to produce shear when fluid is in motion [47]. In other words it is a measure of how much force is required to slip from one layer of the fluid to another layer. Usually liquids and gasses have non-zero viscosity [48]. The coefficient of viscosity is denoted by symbol μ .

2.6 Newtonian and non-Newtonian fluid

A fluid in which the stress arising from its flow at every point are linearly proportional to the local strain rate is called Newtonian fluid [46]. Newtonian fluid behaviour is described by the relation

$$\tau = \mu \frac{du}{dy}. \quad (2.6)$$

In above equation τ is the stress tensor, μ is the viscosity and du/dy is the deformation rate. Fluids in which the shear stress is not directly proportional to deformation rate are known as non-Newtonian fluid.

2.6.1 Power-Law Model

There are many proposed models of non-Newtonian fluids. The most common is the power-law model proposed by [46]. The power-law model in one dimensional flow is given as

$$\tau = K \left(\frac{du}{dy} \right)^n, \quad (2.7)$$

where n is called the behaviour index and K is the coefficient of consistency index. The power-law model can be rewritten in the form

$$\tau = K \left| \frac{du}{dy} \right|^{n-1} \frac{du}{dy} = \eta \frac{du}{dy}. \quad (2.8)$$

Here $\eta = K \left| \frac{du}{dy} \right|^{n-1}$ is referred as apparent viscosity. In the above equation $n = 1$ represents the Newtonian behaviour of fluid. For $n < 1$, behaviour of fluid is known as shear-thinning which is categorized by an apparent viscosity which decreases with the increase in shear rate (For details see [49]). However, when $n > 1$ it represents the shear-thickening behavior of fluid characterized by an apparent viscosity which increases with the increasing shear rate (see [49]). Therefore, a single parameter n describes the nature of fluid behavior.

2.7 Generalized Continuity Equation

Continuity equation is constructed by law of conservation of mass which states that mass can neither be created nor destroyed inside a control volume. If we consider a differential control volume system enclosed by a surface fixed in space, then the mass inside the fixed

control system will not change. Then the equation of continuity can be expressed as

$$\frac{\partial \rho}{\partial t} + \nabla \cdot (\rho \mathbf{V}) = 0. \quad (2.9)$$

If the density is constant and spatially uniform, in that case Eq.(2.9) become

$$\nabla \cdot \mathbf{V} = 0. \quad (2.10)$$

2.8 The Momentum Equation

The equation of linear momentum for fluid particle is obtained from the Newton's second law of motion which states that: "the net force acting on a fluid particle is equal to the time rate of change of linear momentum." Consider the mass in a system defined by control surface of infinitesimally small dimensions dx , dy and dz . The mass of the system is constant, therefore Newtons second law can be written as

$$m \frac{D\mathbf{V}}{Dt} = F. \quad (2.11)$$

The flow of the fluid is represented by the differential equation as

$$\rho \frac{D\mathbf{V}}{Dt} = \nabla \cdot \boldsymbol{\tau} + \rho \mathbf{b}, \quad (2.12)$$

where $\rho \mathbf{b}$ is the body force per unit mass, $\nabla \cdot \boldsymbol{\tau}$ is the surface forces and $\boldsymbol{\tau}$ is the Cauchy stress tensor.

2.8.1 Magnetohydrodynamics

Magnetohydrodynamics (MHD) is the branch of engineering in which the behaviour of magnetic field in electrically conducting fields are studied. The word magnetohydrodynamics is derived from magneto meaning magnetic field, hydro meaning liquid and

dynamics meaning movement. The set of equations which represents MHD are a combination of the equations of motion in fluid dynamics and the Maxwell's equation of electromagnetism. The fluid dynamical attitude of MHD are managed by adding an electromagnetic force term to the equation of motion. The momentum equation with electromagnetic force term is

$$\rho \frac{D\mathbf{V}}{Dt} = \nabla \cdot \boldsymbol{\tau} + (\mathbf{J} \times \mathbf{B}). \quad (2.13)$$

In the above equation \mathbf{J} is the current density and $\mathbf{B} = \mathbf{B} + \mathbf{B}_1$ is the total magnetic field where \mathbf{B}_1 is induced magnetic field considered to be negligible in comparison with external magnetic field which is justified for MHD flow at small magnetic Reynolds number. By Ohm's law [50], we have

$$\mathbf{J} = \sigma(\mathbf{E} + \mathbf{V} \times \mathbf{B}), \quad (2.14)$$

where σ is the electrical conductivity, \mathbf{E} is the electric field. The imposed and induced electrical fields are assumed to be negligible. The electromagnetic force term $\mathbf{J} \times \mathbf{B}$ can be simplified to

$$\mathbf{J} \times \mathbf{B} = -\sigma \mathbf{B}^2 \mathbf{V}. \quad (2.15)$$

It is assumed that the electric field due to polarization of charges is also negligible. Thus momentum equation (2.12) with MHD becomes

$$\rho \frac{D\mathbf{V}}{Dt} = \nabla \cdot \boldsymbol{\tau} - \rho \sigma \mathbf{B}^2 \mathbf{V}. \quad (2.16)$$

2.8.2 Porosity

The porosity is the ratio of volume of pores (empty space) to the bulk volume of a porous medium. A porous medium is often identified by its porosity [47]. The momentum

equation (2.12) with porosity and MHD is as follows

$$\rho \frac{D\mathbf{V}}{Dt} = \nabla \cdot \boldsymbol{\tau} - \rho \sigma \mathbf{B}^2 \mathbf{V} - \rho k \mathbf{V}. \quad (2.17)$$

Here k is the porosity of the medium.

2.9 Heat Transfer

Heat transfer is the energy transfer due to temperature difference. When there is a temperature difference in a medium or between media, heat transfer must take place.

Heat transfer can occur through three mechanism: conduction, convection and radiation.

2.9.1 Conduction

Conduction is the mode of energy transfer by the movement of particles that are interacted with each other, typically in a solid or liquid. The word “conduction” is repeatedly used to describe three different kinds of behavior: Heat Conduction (or Thermal Conduction) - The conduction of heat through direct interaction, such as when you touch the handle of a hot metal skillet. Electrical Conduction - The conduction of electrical current, like through the wires in your house. Sound Conduction (or Acoustic Conduction) - The conduction of sound waves, for example feeling the vibrations of music through a wall. Fourier determined that heat transfer per unit area is directly proportional to temperature gradient and constant of proportionality is then called thermal conductivity. i.e.

$$\frac{Q}{A} = -\kappa \frac{dT}{dA}. \quad (2.18)$$

Here Q is the rate of heat transfer, A is the area, κ is the thermal conductivity and dT/dA is the temperature gradient. This is known as Fourier law.

2.9.2 Convection

Convection is the transfer of heat through fluids (gases or liquids) from a warmer place to a cooler place. In fluid dynamics, convection is the energy transfer due to bulk fluid motion. Convective heat transfer arises between a fluid in a motion and a bounding surface. If there is a difference in the temperature of fluid and bounding surface then thermal boundary layer is created. Fluid particles which interact with the surface attain equilibrium at the surface temperature and transfer energy in the next layer and so on. Through this mode, temperature gradients are produced in fluid. Therefore, the area of fluid containing these temperature gradients are identified as thermal boundary layer. Since the convective heat transfer is by both random molecular motion and the bulk motion of fluid, the molecular motion is more adjacent to the surface where the fluid velocity is less. Convective heat transfer depends upon the nature of the flow. Therefore convection has three forms: Forced convection, Natural (free) convection, Mixed convection. Forced convection is a process, or kind of energy transfer in which fluid motion is produced by an external source. It should be deliberated as one of the core techniques of useful heat transfer as a weighted amount of heat energy can be transferred very efficiently. Natural(free) convection is a heat transport process, in which the fluid motion is not developed by any external source, but only by density differences in the fluid taking place due to temperature gradients. Mixed convection is combined forced convection and

natural convection, occurs when natural convection and forced convection act collectively to transfer heat. This is also defined as the circumstances where both pressure forces and buoyant forces act together. Irrespective of the specific nature of the convective heat transfer mechanism is represented by the equation known as Newton's law of cooling is:

$$\frac{Q}{A} = h(T_s - T_f), \quad (2.19)$$

where h is the heat transfer coefficient, T_s is the temperature of the object's surface and interior, and T_f is the temperature of the environment i.e. the temperature suitably far from the surface.

2.9.3 Radiation

Radiation is the energy transfer due to release/discharge of electromagnetic waves or photons from a surface volume. Radiation doesn't require any medium to transfer heat. The energy produced by radiation is transformed by electromagnetic waves.

2.10 Energy Equation

The first law of thermodynamics expresses the energy equation according to which rate of change of energy inside the fluid element is equals to the rate of workdone on the element due to body or surface force and the sum of net heat flux of fluid element. The generalized energy equation is ([51])

$$\rho C_p \left(\frac{DT}{Dt} \right) = \nabla \cdot (\kappa \nabla T) + f \cdot \mathbf{V}. \quad (2.20)$$

Here C_p is the specific heat and f is the body or surface force.

2.11 Mass Transfer

The subject of mass transfer studies the relative motion of some chemical species with respect to others which are driven by concentration gradients. We can say that mass transfer is mass in transport as the result of a species concentration difference in a mixture. The driving potential is provided by species concentration gradient in a mixture for transport of that species. Mass transfer by diffusion is same as heat transfer by conduction [52]. Transfer of heat and mass are kinetic processes that may occur and be studied separately or jointly. Studying them separately is simpler, but it is most convenient to realise that both processes are modelled by similar mathematical equations in the case of diffusion and convection, thus it is more efficient to consider them jointly.

2.11.1 Concentration Equation

Concentration is the ratio of mass of a substance to the total volume of a mixture. The concentration equation can be derived by using Fick's law and law of conservation of species. In a moving fluid, when heat and mass transfer occur simultaneously the relations between the fluxes and the driving potentials are of more complex nature. In this case the concentration equation has a form

$$\rho \frac{DC}{Dt} = D_M(\nabla^2 C) + D_T(\nabla^2 T), \quad (2.21)$$

where D_M is the molecular diffusivity and D_T is the thermal diffusivity.

Chapter 3

Slip effects on flow and heat transfer of MHD power-law fluid by a porous sheet with variable thermal conductivity and thermal radiation

3.1 Introduction

In this chapter we examine the slip effects on heat transfer of MHD boundary layer flow of power-law fluid over a permeable plate embedded in a uniform porous medium with variable thermal conductivity and thermal radiation. In next section we modeled the flow equations and the resulting constitutive equations are then transformed into a system of non-linear ordinary differential equations by applying a suitable similarity

transformation. In section 3.3 the modeled ODEs are solved numerically by using Matlab bvp4c code. Finally the numerical results are discussed at the end of the chapter for various parameters affecting flow and heat transfer.

3.2 Mathematical Modeling

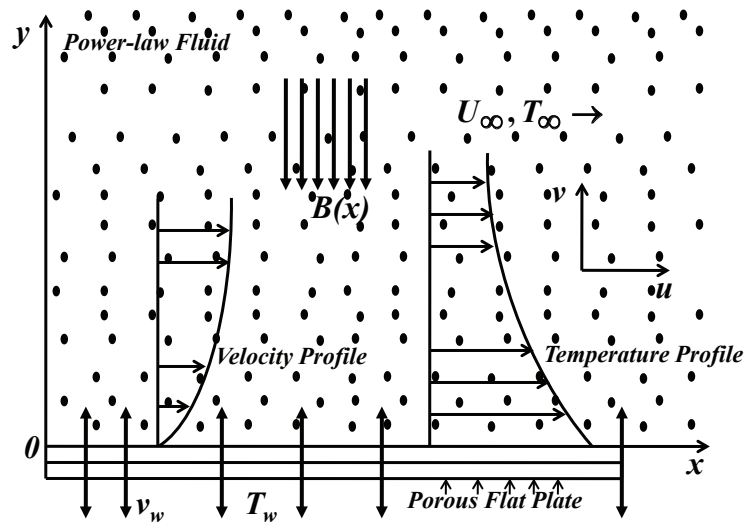


Figure 3.1: Geometry of the problem

Consider the steady two-dimensional laminar flow with heat transfer of an incompressible power-law fluid under the influence of magnetic field B and thermal radiation, over a semi-infinite porous plate in a porous medium. The surface of the plate is insulated and admits partial slip condition. The leading edge of the plate is at $x = 0$ and coincide with the plane $y = 0$. The temperature of the plate is T_w and the flow far away from the plate is uniform and in the direction parallel to the plate. The velocity and temperature far away from the plate are U_∞ and T_∞ respectively. The geometry of the flow problem

is given in figure (3.1) The governing equations for the flow model are given in Eqs. 2.10, 2.20 and 2.21, which under boundary layer approximation along with the slip boundary conditions can be written as

$$\frac{\partial u}{\partial x} + \frac{\partial v}{\partial y} = 0, \quad (3.1)$$

$$u \frac{\partial u}{\partial x} + v \frac{\partial u}{\partial y} = \frac{1}{\rho} \frac{\partial \tau_{xy}}{\partial y} - \frac{1}{\rho A} (u - U_\infty) - \frac{\sigma B^2}{\rho} (u - U_\infty), \quad (3.2)$$

$$u \frac{\partial T}{\partial x} + v \frac{\partial T}{\partial y} = \frac{1}{\rho C_p} \left(\frac{\partial}{\partial y} (\kappa(T) \frac{\partial T}{\partial y}) - \frac{\partial q_r}{\partial y} \right), \quad (3.3)$$

$$u = L_1 \left(\frac{\partial u}{\partial y} \right), \quad v = v_w; \quad T = T_w + D_1 \left(\frac{\partial T}{\partial y} \right); \quad \text{at } y = 0, \quad (3.4)$$

$$u \rightarrow U_\infty, \quad T \rightarrow T_\infty, \quad \text{as } y \rightarrow \infty. \quad (3.5)$$

In the above equations u and v are the velocity components in x and y directions, ρ is the fluids density, τ_{xy} is the component of shear stress tensor, A is the permeability, σ is the electrical conductivity, B is the applied magnetic field, T is the temperature, C_p is the specific heat, κ is the variable thermal conductivity, q_r is the radiative heat flux, L_1 is the velocity slip factor, D_1 is the thermal slip factor and v_w describe suction/blowing through the porous plate. The shear stress component τ_{xy} for the power-law model as derived by Bird et al. [49] is given as

$$\tau_{xy} = K \left| \frac{\partial u}{\partial y} \right|^{n-1} \frac{\partial u}{\partial y}. \quad (3.6)$$

Here K is the consistency coefficient and n is the power-law index. Substitution of Eq.(3.6) in Eq.(3.2) gives

$$u \frac{\partial u}{\partial x} + v \frac{\partial u}{\partial y} = \frac{1}{\rho} \frac{\partial}{\partial y} \left(K \left| \frac{\partial u}{\partial y} \right|^{n-1} \frac{\partial u}{\partial y} \right) - \frac{1}{\rho A} (u - U_\infty) - \frac{\sigma B^2}{\rho} (u - U_\infty). \quad (3.7)$$

Following [45], we consider the temperature-dependent thermal conductivity and radiative heat flux of the form

$$\kappa = \kappa_{\infty} \left(1 + \epsilon \frac{T - T_{\infty}}{\Delta T} \right), \quad (3.8)$$

$$q_r = - \frac{4\sigma^*}{3k^*} \frac{\partial T^4}{\partial y}, \quad (3.9)$$

where ϵ is the thermal conductivity parameter, κ_{∞} is the thermal conductivity at ambient temperature and $\Delta T = T_w - T_{\infty}$, σ^* is the Stefan-Boltzmann constant and k^* is the mean absorption coefficient. It is assumed that the temperature differences within the flow is such that T^4 can be represented as a linear combination of the temperature. Therefore expanding T^4 in Taylor's series about T_{∞} and considering only the linear terms gives us

$$T^4 \cong 4T_{\infty}^3 T - 3T_{\infty}^4. \quad (3.10)$$

Eq. (3.9) together with Eq. (3.10) becomes

$$\frac{\partial q_r}{\partial y} = - \frac{16T_{\infty}^3 \sigma^*}{3k^*} \frac{\partial^2 T}{\partial y^2}. \quad (3.11)$$

Substitution of Eq. (3.8) and Eq. (3.11) into Eq.(3.3) gives

$$u \frac{\partial T}{\partial x} + v \frac{\partial T}{\partial y} = \frac{1}{\rho C_p} \left(\frac{\partial}{\partial y} \left(\kappa_{\infty} \left(1 + \epsilon \frac{T - T_{\infty}}{T_w - T_{\infty}} \right) \frac{\partial T}{\partial y} \right) + \frac{16T_{\infty}^3 \sigma^*}{3k^*} \frac{\partial^2 T}{\partial y^2} \right). \quad (3.12)$$

3.3 Method of Solution

In this section we transform the system of equations (3.1), (3.7) and (3.12) along with the boundary conditions (3.4)-(3.5) into a dimensionless form. For this purpose, the dimensionless stream function $\psi(x, y)$ of the form

$$u = \frac{\partial \psi}{\partial y}, \quad v = - \frac{\partial \psi}{\partial x}, \quad (3.13)$$

identically satisfies the continuity Eq. (3.1). Using Eq. (3.13), Eqs. (3.7) and (3.12)

becomes

$$\frac{\partial \psi}{\partial y} \frac{\partial^2 \psi}{\partial x \partial y} - \frac{\partial \psi}{\partial x} \frac{\partial^2 \psi}{\partial y^2} = \frac{1}{\rho} \left(\frac{\partial}{\partial y} \left[K \left| \frac{\partial^2 \psi}{\partial y^2} \right|^{n-1} \frac{\partial^2 \psi}{\partial y^2} \right] - \left(\frac{1}{\rho k} + \frac{\sigma B^2}{\rho} \right) \left(\frac{\partial \psi}{\partial y} - U_\infty \right) \right), \quad (3.14)$$

$$\frac{\partial \psi}{\partial y} \frac{\partial T}{\partial y} - \frac{\partial \psi}{\partial x} \frac{\partial T}{\partial x} = \frac{1}{\rho C_p} \left(\frac{\partial}{\partial y} \left(\kappa_\infty \left(1 + \epsilon \frac{T - T_\infty}{T_w - T_\infty} \right) \frac{\partial T}{\partial y} \right) + \frac{16 T_\infty^3 \sigma^*}{3 k^*} \frac{\partial^2 T}{\partial y^2} \right). \quad (3.15)$$

The boundary conditions are likewise transformed into

$$\frac{\partial \psi}{\partial y} = L_1 \frac{\partial^2 \psi}{\partial y^2}, \quad \frac{\partial \psi}{\partial x} = -v_w; \quad T = T_w + D_1 \left(\frac{\partial T}{\partial y} \right) \quad \text{at} \quad y = 0, \quad (3.16)$$

$$\frac{\partial \psi}{\partial y} \rightarrow U_\infty, \quad T \rightarrow T_\infty \quad \text{as} \quad y \rightarrow \infty, \quad (3.17)$$

where $L_1 = L \frac{U_\infty \rho}{K} \left(\frac{Kx}{\rho U_\infty^{2-n}} \right)^{\frac{1}{n+1}}$ is the velocity slip factor and $D_1 = D \frac{U_\infty \rho}{K} \left(\frac{Kx}{\rho U_\infty^{2-n}} \right)^{\frac{1}{n+1}}$ is the thermal slip factor with L and D being initial values of velocity and thermal slip parameters respectively.

We introduce of the dimensionless similarity variable

$$\eta = \left(\frac{Re}{x/L} \right)^{\frac{1}{n+1}} \frac{y}{L}, \quad (3.18)$$

where $Re = \rho U_\infty^{2-n} L^n / K$ is the generalized Reynolds number, the dimensionless stream function $\psi(\eta)$ and dimensionless temperature $\theta(\eta)$ of the form

$$\psi(x, y) = LU_\infty \left(\frac{x/L}{Re} \right)^{\frac{1}{n+1}} f(\eta), \quad \theta(\eta) = \frac{T - T_\infty}{T_w - T_\infty}, \quad (3.19)$$

The differential equations (3.14)-(3.15) together with the boundary conditions (3.16)-(3.17) reduced to the form

$$n |f''|^{n-1} f''' + \frac{1}{n+1} f f'' - (k+M)(f' - 1) = 0, \quad (3.20)$$

$$\theta'' + \frac{P_{r\infty}}{(n+1)(1+\epsilon\theta+N_r)} f\theta' + \frac{\epsilon}{(1+\epsilon\theta+N_r)} \theta'^2 = 0, \quad (3.21)$$

$$f(\eta) = S, \quad f'(\eta) = \delta f''(\eta), \quad \theta(\eta) = 1 + \beta\theta'(\eta), \quad \text{at } \eta = 0, \quad (3.22)$$

$$f'(\eta) \rightarrow 1, \quad \theta(\eta) \rightarrow 0, \quad \text{as } \eta \rightarrow \infty. \quad (3.23)$$

In Eqs.(3.20)-(3.23), k is the permeability parameter, M is the magnetic parameter, $P_{r\infty}$ is the local Prandtl number, N_r is the thermal radiation parameter, S is the suction/blowing parameter corresponds to suction when $S > 0$ and corresponds to blowing when $S < 0$. Here δ and β are the dimensionless velocity and thermal slip parameters respectively. These parameters are given by

$$k = \frac{x}{\rho A U_\infty}, \quad (3.24)$$

$$M = \frac{x\sigma B^2}{\rho U_\infty}, \quad (3.25)$$

$$P_{r\infty} = \frac{C_p}{\kappa_\infty} K^{2/n+1} \left(\frac{U_\infty^3 \rho}{x} \right)^{\frac{n-1}{n+1}}, \quad (3.26)$$

$$N_r = \frac{16T_\infty^3 \sigma^*}{3k^* \kappa_\infty}, \quad (3.27)$$

$$S = -v_w \frac{x(n+1)}{U_\infty} \left(\frac{\rho U_\infty^{2-n}}{K} \right)^{\frac{1}{n+1}}, \quad (3.28)$$

$$\delta = L \frac{U_\infty \rho}{K}, \quad (3.29)$$

$$\beta = D \frac{U_\infty \rho}{K}. \quad (3.30)$$

Eq.(3.26) can also be written as

$$P_{r\infty} = (1 + \epsilon\theta) P_r, \quad (3.31)$$

where $P_r = \frac{C_p}{\kappa} \left(\frac{U_\infty^3 \rho}{x} \right)^{\frac{n-1}{n+1}} K^{2/n+1}$ is the Prandtl number. Using Eq.(3.31) the Eq.(3.21)

become

$$\theta'' + \frac{(1 + \epsilon\theta)}{(1 + \epsilon\theta + N_r)} \frac{P_r}{n+1} f\theta' + \frac{\epsilon}{(1 + \epsilon\theta + N_r)} \theta'^2 = 0. \quad (3.32)$$

In order to solve the system of ordinary differential equations (3.20) and (3.32) with boundary conditions (3.22)-(3.23) using Matlab bvp4c code, we have to first convert these equations into a system of first order differential equations, i.e.,

$$f' = p, \quad p' = q, \quad q' = \frac{k + M}{n} \frac{p - 1}{q^{n-1}} - \frac{fq^{2-n}}{n(n+1)}, \quad (3.33)$$

$$\theta' = z, \quad z' = -\frac{Pr}{n+1} \frac{1 + \epsilon\theta}{(1 + \epsilon\theta + Nr)} fz - \frac{\epsilon}{(1 + \epsilon\theta + Nr)} z^2, \quad (3.34)$$

along with the boundary conditions

$$f(\eta) = S, \quad p(\eta) = \delta q(\eta), \quad \text{at } \eta = 0; \quad p(\eta) \rightarrow 1 \quad \text{as } \eta \rightarrow \infty, \quad (3.35)$$

$$\theta(\eta) = 1 + \beta z(\eta), \quad \text{at } \eta = 0; \quad \theta(\eta) \rightarrow 0 \quad \text{as } \eta \rightarrow \infty. \quad (3.36)$$

The bvp4c solver needs an initial guess for $q(\eta)$ and $z(\eta)$ at $\eta = 0$, and through collocation

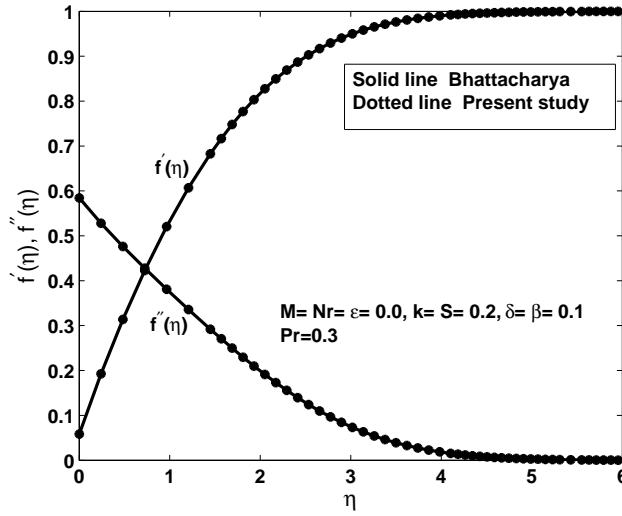


Figure 3.2: Velocity $f'(\eta)$ and shear stress $f''(\eta)$ profiles for $M = \epsilon = N_r = 0$ and $n = 1$.

method we vary each guess until we obtain an appropriate solution for our problem. We verify the accuracy of these solutions by comparing them with those found using shooting method. The result for the velocity profile with $M = 0$ and $n = 1$ (i.e in the absence of

MHD and for the case of Newtonian fluids) are compared with the available published results of [18]. The comparison is presented in figure (3.2).

3.4 Results and Discussion

In this section we discuss the numerical results presented in the form of graphs and tables. The computations are performed for several values of power-law index n and the effects of velocity slip parameter δ , thermal slip parameter β , permeability parameter k , magnetic parameter M , Prandtl number Pr , variable thermal conductivity ϵ and thermal radiation N_r , and hence the effect of these parameters on velocity and temperature profile are discussed.

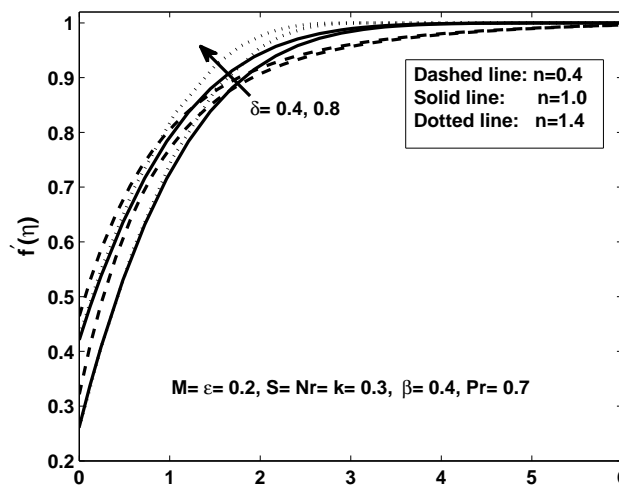


Figure 3.3: Velocity $f'(\eta)$ profiles for different values of slip parameter δ and power-law index n .

In figure (3.3) the effect of velocity slip parameter δ and power-law index n on the velocity profile of Newtonian, shear thinning and shear thickening fluids is presented. The comparison of curves with same power-law index shows that the increase in the velocity

slip at the boundary, increases the fluid velocity within the boundary layer. This is due to the positive value of the fluid velocity adjacent to the surface. Moreover, the increase in magnitude of the slip parameter allow more fluid to slip past the plate and accordingly the flow through the boundary layer will increase. Therefore the thickness of velocity boundary layer to decrease.

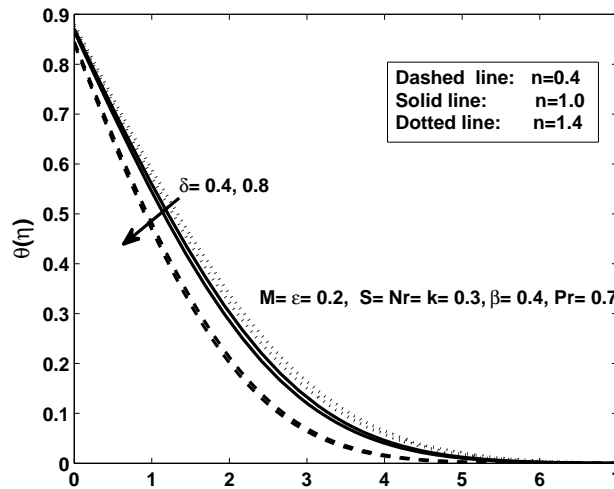


Figure 3.4: Temperature $\theta(\eta)$ profiles for different values of slip parameter δ and power-law index n .

It is important to note that temperature is dependent on velocity in situations where heat transfer is accomplished by convection, as this principle will also be important for following discussions. In figure (3.4) the temperature profile $\theta(\eta)$ is plotted for two different values of velocity slip parameter δ . It is observed that the increase in the magnitude of velocity slip at boundary enhance the rate of heat transfer.

Figures (3.3)-(3.4) with slip parameter $\delta = 0.8$ gives variation of velocity and thermal profiles for both Newtonian and non-Newtonian fluids. It is evident from figure (3.3), initially the velocity of shear-thinning fluid $n < 1$ rises fastest, followed by the shear-thickening fluid $n > 1$ and then the Newtonian fluids $n = 1$. This is due to smallest

effective viscosity of shear thinning fluids at that point. Therefore shear thinning fluids achieve a higher strain rate and velocity. Whereas at later times the velocity of shear thinning fluid, first decrease below the shear thickening fluid and then the Newtonian fluids. This opposite trend is observed due the decrease in shear stress and increase in the viscosity of the shear thinning fluids. Furthermore, figure (3.4) show the thickness of thermal boundary layer is relatively thin for shear thinning fluid $n < 1$ (f approaches zero quickly). However, if $n > 1$ the boundary layer is relatively thick.

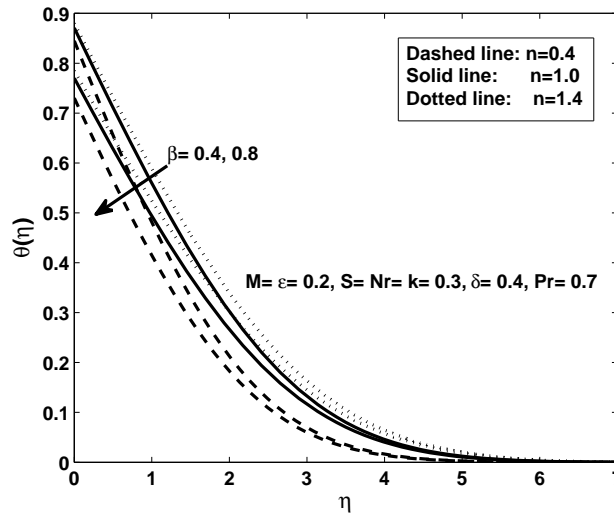


Figure 3.5: Temperature $\theta(\eta)$ profiles for different values of thermal slip parameter β and power-law index n .

The effect of thermal slip parameter β on temperature profile is presented in figure (3.5). The increase in thermal slip parameter decreases the fluid temperature for a given distance from the plate. This is due to the fluid adjacent to the surface of the plate having temperature lower than that of the plate.

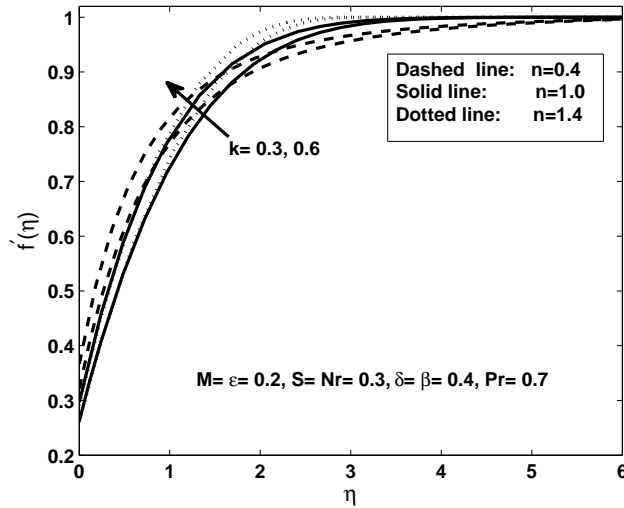


Figure 3.6: Velocity $f'(\eta)$ profiles for different values of permeability parameter k and power-law index n .

In figure (3.6) effect of variation in permeability on fluid velocity with slip parameter is shown. It is noticed that the velocity of the fluid across the boundary layer increase with increase in the permeability of the porous medium. In other words, the increase in the porosity of the medium decreases the magnitude of the Darcian body force which enhances the motion of the fluid in the boundary layer. Figure (3.6) with permeability $k = 0.3$ and different values of the power-law index give variation of velocity profile for Newtonian and non-Newtonian fluids. It is evident from figure (3.6), initially the shear-thinning fluid rises faster when compared with the shear-thickening fluid. This is due to smallest effective viscosity of shear thinning fluids. Whereas the opposite trend is observed at the later times as viscosity of the shear thickening fluid will decrease. Moreover, the slip parameter at the boundary allow more fluid flow past the plate and causes thinning of boundary layer.

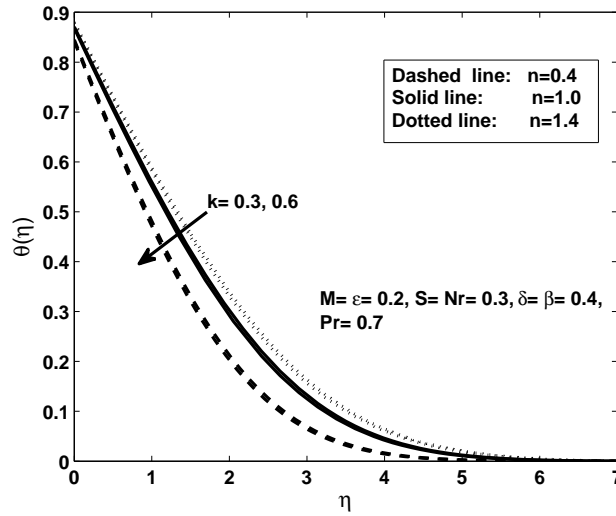


Figure 3.7: Temperature $\theta(\eta)$ profiles for different values of permeability parameter k and power-law index n .

The partial slip and the effect of variation in permeability on temperature profile is presented in figure (3.7). It is observed that the increase in permeability causes to decrease the temperature of the fluid which in turn enhanced the rate of heat transfer and thinning of thermal boundary layer.

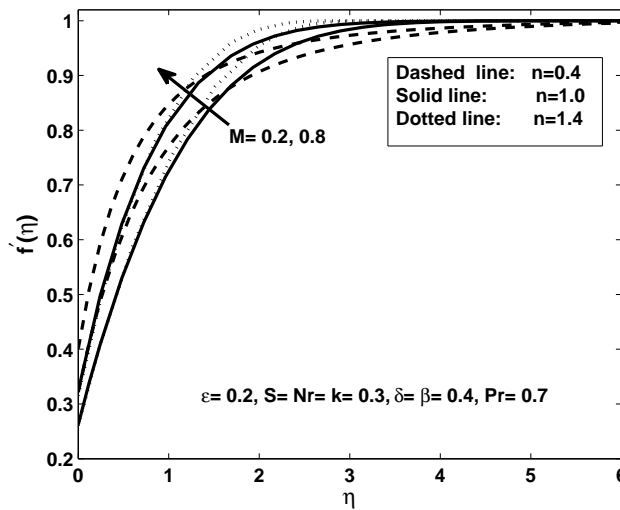


Figure 3.8: Velocity $f'(\eta)$ profiles for different values of magnetic parameter M and power-law index n .

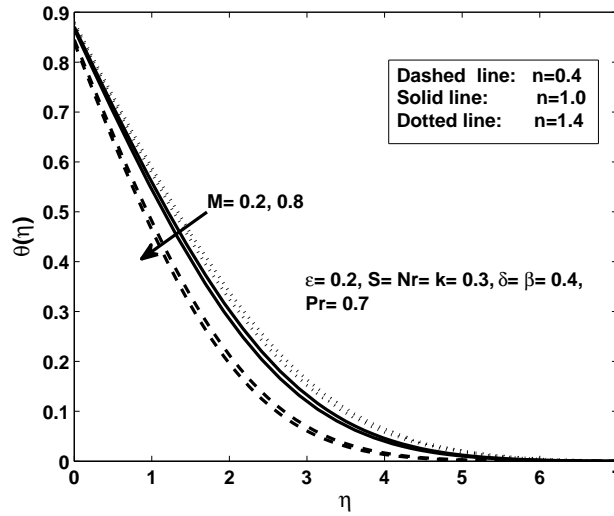


Figure 3.9: Temperature $\theta(\eta)$ profiles for different values of magnetic parameter M and power-law index n .

The effects of MHD parameter M on fluid velocity and temperature under slip condition is shown in figures (3.8)-(3.9). It is clear that the variation in MHD parameter M show the similar effect as variation in permeability parameter k , i.e., the increase in magnetic field caused an increase in velocity of the fluid and the rate of heat transfer.

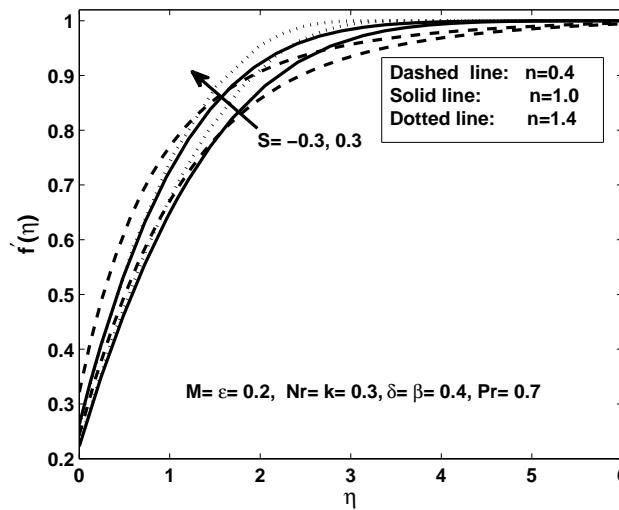


Figure 3.10: Velocity $f'(\eta)$ profile for different values of suction/injection parameter S and power-law index n .

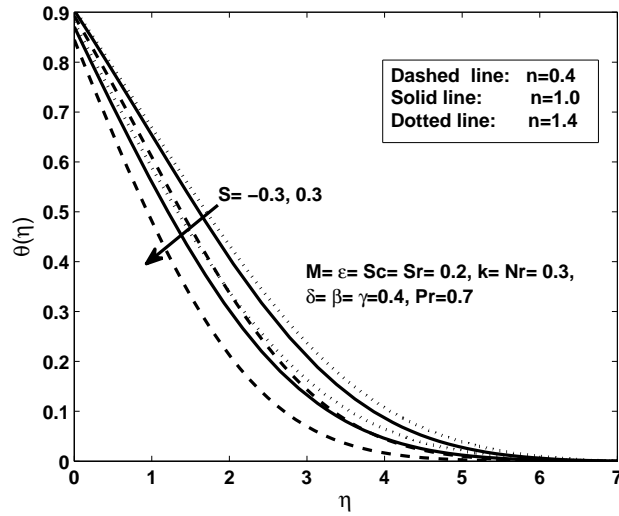


Figure 3.11: Temperature $\theta(\eta)$ profiles for different values of suction/injection parameter S and power-law index n .

Figures (3.10)-(3.11) depicted the effect of suction/injection parameter S on velocity and temperature profile in the presence of slip condition and magnetic field for porous plate in a porous medium. It is clear from the figure that suction $S > 0$ caused an increase in fluid velocity as more fluid is sucked through the porous wall. Opposite behaviour is observed for $S < 0$. In case of temperature distribution through the boundary layer, increasing values of $S > 0$ causes the thinning of thermal boundary layer. This will increase the rate of heat transfer through the boundary layer.

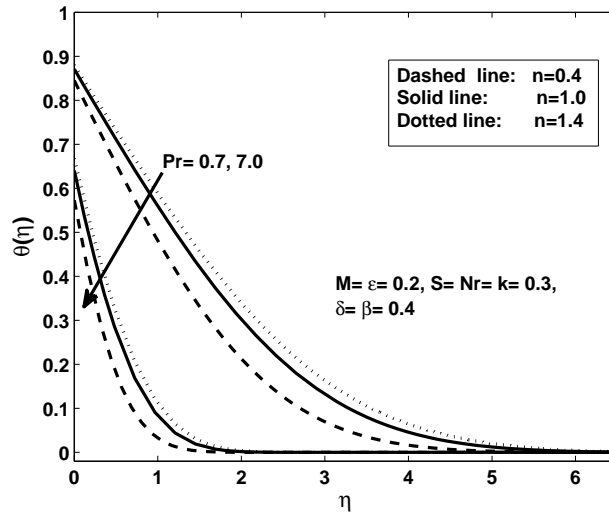


Figure 3.12: Temperature $\theta(\eta)$ profiles for different values of Prandtl number Pr and power-law index n .

Prandtl number is defined as the ratio of momentum diffusivity to thermal diffusivity. Variation in Prandtl number and its effects on the temperature profile is shown in figure (3.12). It is observed that the temperature of the power-law fluid decrease with increasing values of the Prandtl number under slip condition. This trend is consistent with the fact that increase in Prandtl number will increase the fluid viscosity. This will cause a decrease in the velocity flow and the decrease in temperature.

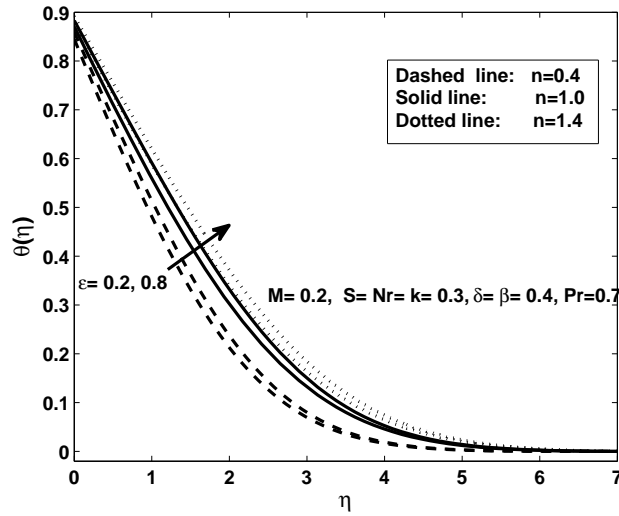


Figure 3.13: Temperature $\theta(\eta)$ profiles for different values of thermal conductivity parameter ϵ and power-law index n .

The temperature profile for various values of thermal conductivity parameter ϵ is shown in figure (3.13). It is noticed that an increase in thermal conductivity parameter, increases the fluid temperature. It would also increase the thermal boundary layer thickness.

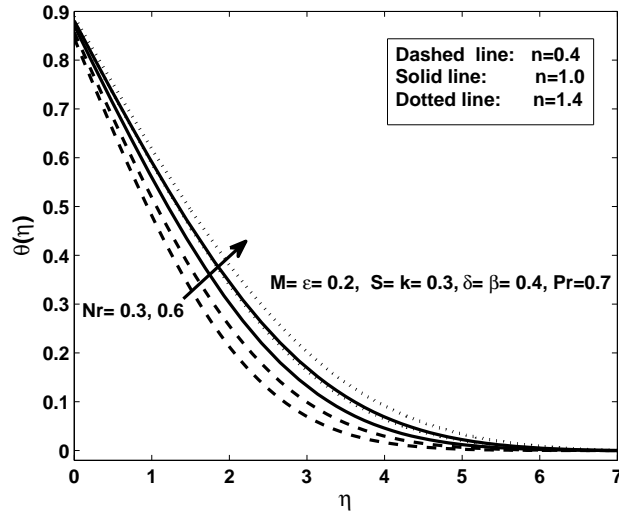


Figure 3.14: Temperature $\theta(\eta)$ profiles for different values of thermal radiation parameter N_r and power-law index n .

Figure (3.14) illustrates the effect of thermal radiation parameter N_r on temperature profile. We see that an increase in thermal radiation parameter increases the temperature of the power-law fluid. From figure (3.14) it is also noticed, the thickness of thermal boundary layer increase with increase in power-law index n .

Table 3.1: Values of skin friction coefficient $f''(0)$

n	k	M	δ	$f''(0)$
0.4	0.3	0.6	0.3	1.036
1.0				0.8114
1.4				0.7861
1.4	0.3	0.6	0.3	0.7861
	0.6			0.8629
	0.8			0.9001
1.4	0.3	0.2	0.3	0.6718
		0.6		0.7861
		1.0		0.8712
1.4	0.3	0.6	0.0	0.9667
			0.3	0.7861
			0.6	0.656

Table 3.1 presents the nature of skin friction coefficient for different physical parameters. It is observed, the shear thinning fluids have the highest value of skin friction coefficient followed by the Newtonian fluid and then the shear thickening fluids. This

is because the fact that the rate of increase in velocity at the surface of porous plate is highest for shear thinning fluids. Moreover, the skin friction coefficient decrease with increase in slip parameter δ and increase with increase in magnetic parameter M . The increasing values of skin friction coefficient corresponds to thinning of velocity boundary layer. Whereas the decreasing values of skin friction coefficient corresponds to fluid velocity at the surface approaching to free stream velocity.

Nusselt number is the ratio of convective to conductive heat transfer at the surface of the plate. In table 3.2 different values of Nusselt number are presented when all other parameters are kept constant. It is observed that the Nusselt number decrease with increase in power-law index n . This observation is consistent with the fact that the decrease in surface temperature is slowest for shear thickening fluids. It can be noticed from the table that an increase in the permeability parameter k , magnetic parameter M and Prandtl number P_r results in an increase in Nusselt number. Increase in the slip parameters δ and β has the effect of lowering the Nusselt number. The thermal radiation parameter N_r gives the same effect as found for slip parameters. The effect of increase in Nusselt number is analogous to an increase in heat transfer rate and thinning of thermal boundary layer.

Table 3.2: Values of Nusselt number $-\theta'(0)$

n	k	M	δ	β	P_r	N_r	$-\theta'(0)$
0.4	0.3	0.2	0.3	0.3	0.7	0.2	0.3879
1.0							0.3231
1.4							0.3006
1.4	0.6	0.2	0.3	0.3	0.7	0.2	0.307
	0.8						0.3102
1.4	0.3	0.4	0.3	0.3	0.7	0.2	0.3052
		0.8					0.3116
1.4	0.3	0.2	0.6	0.3	0.7	0.2	0.3127
			0.8				0.3186
1.4	0.3	0.2	0.3	0.6	0.7	0.2	0.2768
				0.8			0.2629
1.4	0.3	0.2	0.3	0.3	3.0	0.2	0.5659
					7.0		0.8234
1.4	0.3	0.2	0.3	0.3	0.7	0.4	0.2846
						0.8	0.2603

Chapter 4

Slip effects on flow, heat and mass transfer of MHD power-law fluid by a porous sheet with variable thermal conductivity and thermal radiation

4.1 Introduction

In this chapter we extend the model presented in previous chapter by including the mass transfer to the problem. We will examine the slip effects on mass transfer of MHD boundary layer flow of power-law fluid over the porous plate embedded in a porous medium with variable thermal conductivity and thermal radiation.

4.2 Mathematical Modeling

In addition to Eqs. (3.1)-(3.5), the present model include boundary layer concentration equation with slip conditions. Equation (2.21) under boundary layer approximation can be written as

$$u \frac{\partial C}{\partial x} + v \frac{\partial C}{\partial y} = D_M \frac{\partial^2 C}{\partial y^2} + D_T \frac{\partial^2 T}{\partial y^2}, \quad (4.1)$$

where C is the ambient concentration of the fluid, D_M is the molecular diffusivity and D_T is the thermal diffusivity. The slip boundary conditions are

$$C = C_w + N_1 \left(\frac{\partial C}{\partial y} \right) \quad \text{at } y = 0, \quad (4.2)$$

$$C \rightarrow C_\infty \quad \text{as } y \rightarrow \infty. \quad (4.3)$$

Here C_w is the concentration of the plate, C_∞ is the concentration far away from the plate and N_1 is the mass slip factor.

4.3 Method of Solution

In this section we transform the Eq. (4.1) along with boundary conditions (4.2)-(4.3) into a dimensionless form. Introduction of dimensionless stream function $\psi(x, y)$ given in Eq. (3.13) into Eq. (4.1) gives

$$\frac{\partial \psi}{\partial y} \frac{\partial C}{\partial x} - \frac{\partial \psi}{\partial x} \frac{\partial C}{\partial y} = D_M \frac{\partial^2 C}{\partial y^2} + D_T \frac{\partial^2 T}{\partial y^2}. \quad (4.4)$$

Similarly the boundary conditions are transformed into

$$C = C_w + N_1 \left(\frac{\partial C}{\partial y} \right) \quad \text{at } y = 0, \quad (4.5)$$

$$C \rightarrow C_\infty \quad \text{as } y \rightarrow \infty. \quad (4.6)$$

Here $N_1 = N \frac{U_\infty \rho}{K} \left(\frac{Kx}{\rho U_\infty^{2-n}} \right)^{\frac{1}{n+1}}$ is the mass slip factor with N being initial values of mass slip parameter.

The dimensionless concentration $\phi(\eta)$, defined as

$$\phi(\eta) = \frac{C - C_\infty}{C_w - C_\infty}, \quad (4.7)$$

transformed Eq. (4.4) into the form

$$\phi'' + \frac{S_{c\infty}}{n+1} \phi' f + S_{c\infty} S_{r\infty} \theta'' = 0, \quad (4.8)$$

where $S_{c\infty} = \frac{1}{D_M} \left(\frac{K}{\rho} \right)^{\frac{2}{n+1}} \left(\frac{U_\infty^3}{x} \right)^{\frac{n-1}{n+1}}$ is the Schmidt number and

$S_{r\infty} = D_T \left(\frac{\rho}{K} \right)^{\frac{2}{n+1}} \left(\frac{x}{U_\infty^3} \right)^{\frac{n-1}{n+1}} \frac{T_w - T_\infty}{C_w - C_\infty}$ is the Sorrent number. The boundary conditions

(4.2)-(4.3) are likewise transformed into

$$\phi(\eta) = 1 + \gamma \phi'(\eta), \quad \text{at } \eta = 0, \quad (4.9)$$

$$\phi(\eta) \rightarrow 0 \quad \text{as } \eta \rightarrow \infty. \quad (4.10)$$

Here $\gamma = N \frac{U_\infty \rho}{K}$ is the mass slip parameter. The governing partial differential equation for the present model are (3.20), (3.32) and (4.8) along with the boundary conditions (3.22), (3.23), (4.9) and (4.10). In order to solve the system of equations with Matlab bvp4c code, we convert these equations into the system of first order differential equations:

$$\begin{aligned} f' &= p, & p' &= q, & q' &= \frac{k + M}{n} \frac{p - 1}{q^{n-1}} - \frac{f q^{2-n}}{n(n+1)}, \\ \theta' &= z, & z' &= -\frac{P_r}{n+1} \frac{1 + \epsilon \theta}{(1 + \epsilon \theta - N_r)} f z - \frac{\epsilon}{(1 + \epsilon \theta - N_r)} z^2, \\ \phi' &= t, & t' &= -\frac{S_{c\infty}}{n+1} t f + S_{c\infty} S_{r\infty} z', \end{aligned} \quad (4.11)$$

$$f(\eta) = S, \quad p(\eta) = \delta q(\eta), \quad \text{at } \eta = 0; \quad p(\eta) \rightarrow 1 \quad \text{as } \eta \rightarrow \infty, \quad (4.12)$$

$$\theta(\eta) = 1 + \beta z(\eta), \quad \text{at } \eta = 0; \quad \theta(\eta) \rightarrow 0 \quad \text{as } \eta \rightarrow \infty, \quad (4.13)$$

$$\phi(\eta) = 1 + \gamma t(\eta), \quad \text{at } \eta = 0; \quad \phi(\eta) \rightarrow 0 \quad \text{as } \eta \rightarrow \infty. \quad (4.14)$$

4.4 Results and Discussion

In this section we discuss the numerical results presented in the form of graphs. The calculations are performed for different values of power-law index n and effects of velocity slip parameter δ , thermal slip parameter β , mass slip parameter γ , permeability parameter k , magnetic parameter M , Prandtl number Pr , variable thermal conductivity ϵ , thermal radiation N_r , Schmidt number $S_{c\infty}$ and Soret number $S_{r\infty}$ on velocity, temperature and concentration profiles are discussed.

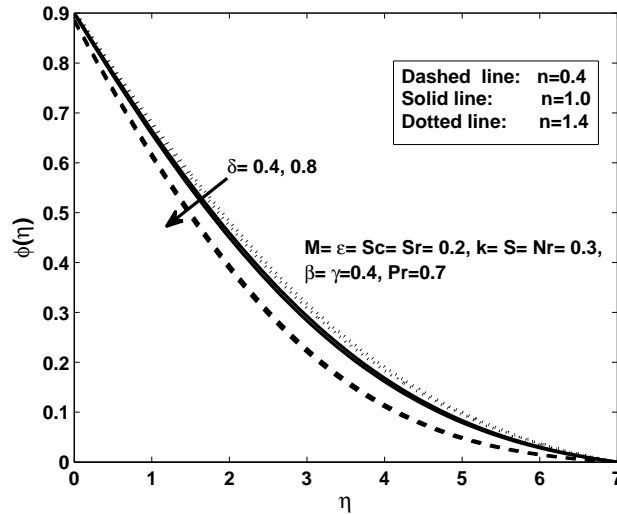


Figure 4.1: Concentration $\phi(\eta)$ profiles for different values of velocity slip parameter δ and power-law index n .

In figure (4.1) the effect of velocity slip parameter δ on concentration profiles of

Newtonian, shear thinning and shear thickening fluids is presented. It can be noticed that an increase in the magnitude of velocity slip at boundary enhances the rate of mass transfer. Figure (4.1) also shows that the boundary layer thickness for shear thinning fluid ($n < 1$) is relatively thin. as compared to shear thickening fluids ($n > 1$).

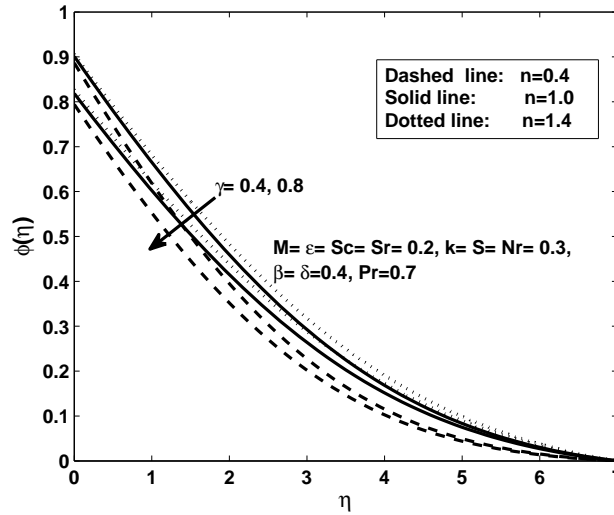


Figure 4.2: Concentration $\phi(\eta)$ profiles for different values of velocity slip parameter γ and power-law index n .

The effect of mass slip parameter γ on concentration profiles with different values of power-law index n is depicted in figure (4.2). The increase in mass slip shows the decrease in concentration profile. This is due to an increase in the mass transfer from the fluid to the porous plate.

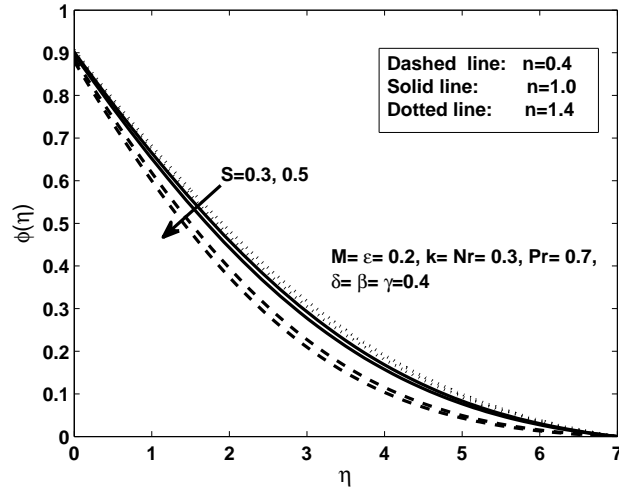


Figure 4.3: Concentration $\phi(\eta)$ profiles for different values of suction parameter S and power-law index n .

The variation in suction parameter with various values of power law index n is shown in figure (4.3) for concentration profiles. The concentration boundary layer decreases with an increase in suction $S > 0$. This will enhance the rate of mass transfer through boundary layer. An opposite behaviour can be seen for blowing $S < 0$.

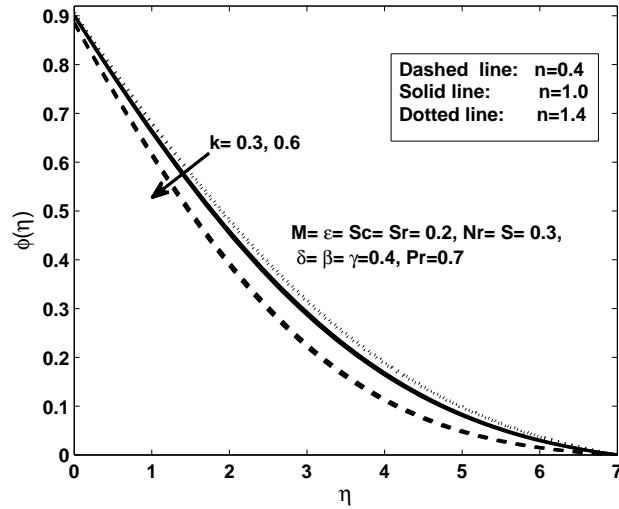


Figure 4.4: Concentration $\phi(\eta)$ profiles for different values of permeability parameter k and power-law index n .

In figure (4.4) the concentration profiles are presented for different values of permeability parameter k . The effects of permeability on velocity and temperature are same as depicted in previous chapter (see figures (3.6)-(3.7)). Here we observed that the concentration of the power-law fluid decreases for an increase in permeability. When the permeability of the porous medium increases the porous medium become more porous which causes the decrease in Darcian body force and the rate of mass transfer is increased in the porous medium.

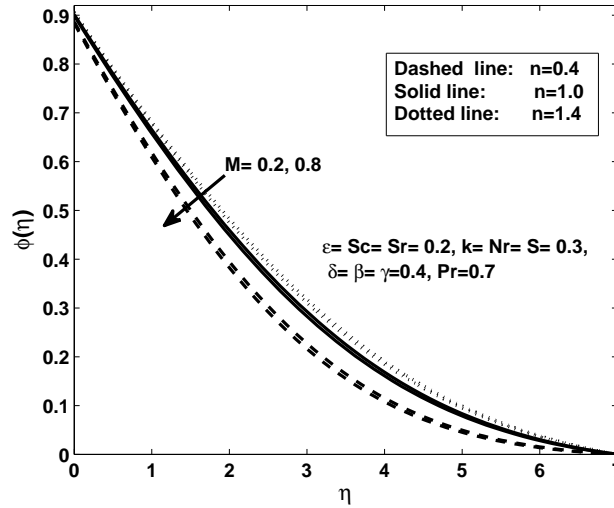


Figure 4.5: Concentration $\phi(\eta)$ profiles for different values of magnetic parameter M and power-law index n .

In figure (4.5) variation of MHD parameter for different values of power-law index n are depicted. It is clear from the figure that the effect of MHD parameter shows the same results as observed for variation in permeability k , i.e., the increase in magnetic field enhances the rate of mass transfer. This is due to the transverse magnetic field a drag force is developed that opposes flow.

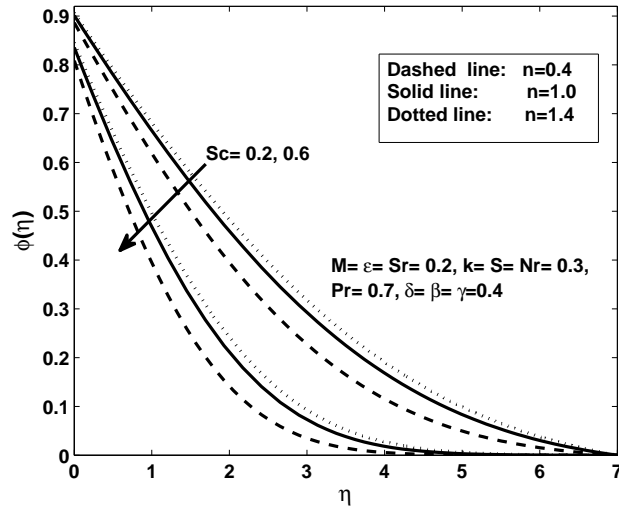


Figure 4.6: Concentration $\phi(\eta)$ profiles for different values of Schmidt number S_c and power-law index n .

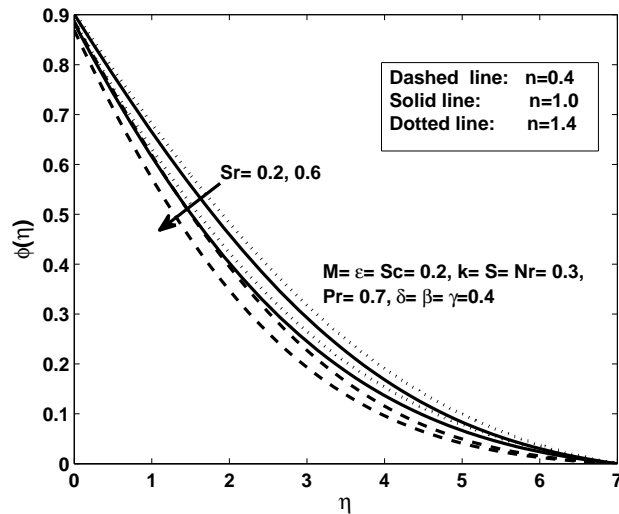


Figure 4.7: Concentration $\phi(\eta)$ profiles for different values of Soret number S_r and power-law index n .

Figure (4.6) illustrate the effect of Schmidt number for various values of power-law index n on concentration profiles. The Schmidt number is the important parameter in the mass transfer process as it describes the ratio of thickness of the viscous and concentration boundary layers. Its effects on species concentration boundary layer is

analogous to the effect of Prandtl number on thermal boundary layer thickness. That is, increase in Schmidt number causes the decrease in concentration profiles and in turn decreases the species concentration boundary layer thickness. We observe the similar behaviour due to the change in Soret number. The decrease in concentration causes an increase in the mass transfer from the fluid to the porous medium as seen in figure (4.7).

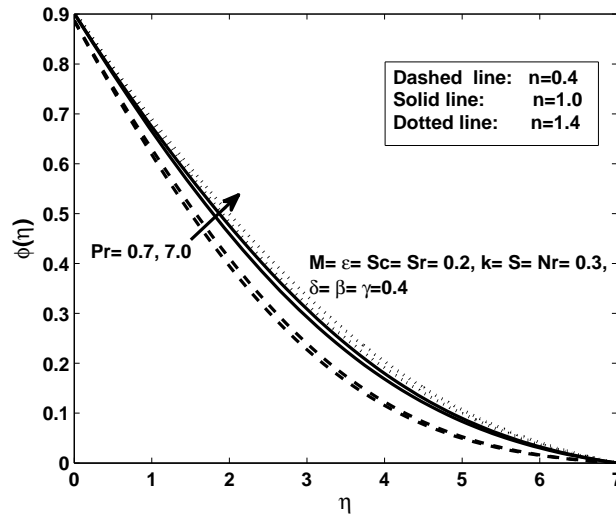


Figure 4.8: Concentration $\phi(\eta)$ profiles for different values of Prandtl number P_r and power-law index n .

In figure (4.8) the effect of Prandtl number on concentration profile is depicted. It is clear from the figure that the increase in Prandtl number caused an increase in concentration and decreases the specie concentration boundary layer.

Chapter 5

Conclusion

In this thesis, we studied the MHD slip flow with heat and mass transfer of power-law fluid over a porous flat plate with variable thermal conductivity and thermal radiation. The velocity, thermal and mass slip conditions are employed and thermal conductivity is considered as linear function of temperature. The governing boundary layer equations along with the boundary conditions were transformed into a coupled system of nonlinear ordinary differential equations using similarity transformation. The resulting system of differential equations was solved numerically using Matlab bvp4c code and results are presented in the form of graphs and tables.

In general, the increase in velocity slip at the boundary, increase the fluid velocity and enhanced the heat and mass transfer rate across the boundary layer. The increase in thermal and mass slip parameter decrease the fluid temperature and concentration for a given distance from the plate. The increase in permeability and MHD parameter resulted an increase in velocity and enhances the rate of heat and mass transfer. Finally, the suction $S > 0$ caused an increase in fluid velocity as more fluid is sucked through the porous

wall and reduce the thickness of momentum and species concentration boundary layer. Opposite behaviour is observed for $S < 0$. In case of temperature and concentration distribution the thermal and species concentration boundary layer thickness decreases with increasing values of $S > 0$. It is observed, the velocity and temperature of power-law fluid decrease with the increasing values of the Prandtl number. Whereas the species concentration of the power-law fluid increase with increasing values of Prandtl number. The increase in thermal radiation parameter resulted in increase in the thickness of thermal boundary layer. The fluid velocity and concentration is unaffected by variations in thermal conductivity and radiation.

The present model has exploited a number of simplifications in order to focus on the principal effects of slip parameter and power-law index and temperature dependent thermal conductivity. An interesting area to explore in future investigations would be the use of temperature dependent viscosity, variable porosity and multidimensional MHD slip flow and heat transfer of non-Newtonian fluids. Clearly there is an opportunity for experimental work on these systems.

References

- [1] L. Prandtl, “Über flussigkeitsbewegungen bei sehr kleiner reibung,” *International Mathematics Kongr. Heidelberg*, pp. 484–491, 1904.
- [2] H. Blasius, “Grenzschichten in flüssigkeiten mit kleiner reibung,” *Z. Math. Phys.*, vol. 56, p. 1, 1908.
- [3] J. P. Pascal and H. Pascal, “Some similarity solutions to shear flows of non-newtonian power law fluids,” *Acta Mechanica*, vol. 112, pp. 229–236, 1994.
- [4] A. M. Abussita, “A note on a certain boundary layer equation,” *Applied Mathematics and Computation*, vol. 64, p. 73, 1994.
- [5] A. Aziz, “A similarity solution for laminar thermal boundary layer flow over a flat plate with a convective surface boundary condition,” *Communications in Nonlinear Science and Numerical Simulation*, vol. 14, p. 1064, 2009.
- [6] A. Ishak, “Similarity solutions for flow and heat transfer over a permeable surface with convective boundary conditions,” *Applied Mathematics and Computation*, vol. 217, p. 837, 2010.

- [7] E. Magyari, “Comment on similarity solution for laminar thermal boundary layer flow over a flat plate with a convective surface boundary condition by a. aziz,” *Communications in Nonlinear Science and Numerical Simulation*, vol. 16, p. 599, 2011.
- [8] K. Vafai, *Handbook of Porous Media*. New York: Marcel Dekker, 2000.
- [9] D. A. Nield and A. Bejan, *Convection in Porous Media*. New York: Springer, 1998.
- [10] D. B. Ingham and I. Pop, *Transport Phenomena in Porous Media*. New York: Pergamon, Elsevier, 1998.
- [11] M. Kumari, I. Pop, and G. Nath, “Non-darcian effects on forced convection heat transfer over a flat plate in a highly porous medium,” *Acta Mechanica*, vol. 84, p. 201, 1990.
- [12] N. Luna and F. Mndez, “Forced convection on a heated horizontal flat plate with finite thermal conductivity in a non-darcian porous medium,” *International Journal of Thermal Sciences*, vol. 44, p. 656, 2005.
- [13] A. R. A. Khaled and K. Vafai, “The role of porous media in modeling flow and heat transfer in biological tissues,” *International Journal of Heat and Mass Transfer*, vol. 46, p. 4989, 2003.
- [14] O. Makinde, “Free convection flow with thermal radiation and mass transfer past a moving porous plate.,” *International Communications in Heat Mass Transfer*, vol. 32, pp. 1411–1419, 2005.

- [15] F. S. Ibrahim, A. M. Elaiw, and A. Bakr, “Influence of viscous dissipation and radiation on unsteady mhd mixed convection flow of micropolar fluids.,” *Applied Mathematics and Information Sciences*, vol. 2, pp. 143–162, 2008.
- [16] M. S. Abel, P. S. Datti, and N. Mahesha, “Flow and heat transfer in a power-law fluid over a stretching sheet with variable thermal conductivity and non-uniform heat source,” *International Journal of Heat and Mass Transfer*, vol. 52, pp. 2901–2913, 2009.
- [17] M. J. Martin and I. D. Boyd, “Momentum and heat transfer in a laminar boundary layer with slip flow,” *Journal of Thermophysics and Heat Transfer*, vol. 20, p. 710, 2006.
- [18] K. Bhattacharrya and S. Mukhopadhyay, “Steady boundary layer slip flow and heat transfer over a flat porous plate embedded in a porous media,” *Journal of petroleum science and Engineering*, vol. 78, p. 304, 2011.
- [19] A. Aziz, J. I. Siddique, and T. Aziz, “Steady boundary layer slip flow along with heat and mass transfer over a flat porous plate embedded in a porous medium,” *PLOS ONE*, 2014.
- [20] D. Pal and B. Talukdar, “Perturbation analysis of unsteady magnetohydrodynamics convective heat and mass transfer in a boundary layer slip flow past a vertical plate with thermal radiation and chemical reaction,” *Communication in Nonlinear science and numerical simulation*, vol. 15, p. 1813, 2010.

- [21] W. A. Khan, Z. H. Khan, and M. Rahi, "Fluid flow and heat transfer of carbon nanotubes along a flat plate with navier slip boundary," *Applied Nanoscience*, vol. 4, pp. 633–641, 2014.
- [22] I. G. Baoku and A. B.I. Olajuwon, "Heat and mass transfer on mhd third grade fluid with partial slip flow past an infinite vertical insulated porous plate in a porous medium," *International Journal of Heat and Mass transfer*, p. 81, 2013.
- [23] T. Wang, "Mixed convection heat transfer from vertical plate to non-newtonian fluids," *International Journal of Heat and Fluid Flow*, vol. 16, pp. 56–61, 1995.
- [24] S. L. H. Xu, "Laminar flow and heat transfer in the boundary layer of non-newtonian fluids over a stretching flat sheet," *Computers and Mathematics with Application*, vol. 57, pp. 1425–1431, 2009.
- [25] C. Cheng, "Soret and dufour effects on free convection boundary layers of non-newtonian power-law fluids with yield stresses in a porous media over a vertical plate with variable wall heat and mass fluxes," *International Communications in Heat and Mass Transfer*, vol. 38, pp. 615–619, 2011.
- [26] A. F. J.B.R Loureiro, "Asymptotic analysis of turbulent boundary layer flow of purely viscous non-newtonian fluids," *Journal of Non-Newtonian Fluid mechanics*, vol. 199, no. 20-28, 2013.
- [27] I. P. H. Xu, SJ Liao, "Series solution of unsteady boundary layer flows of non-newtonian fluids near a forwards stagnation point," *Journal of Non-Newtonian Fluid mechanics*, vol. 139, pp. 31–43, 2006.

- [28] A. K. M. Pakdemirli, M. Yurusoy, “Symmetry groups of boundary layer equations of a class of non-newtonian fluids,” *international journal of Non-linear Mechanics*, vol. 31, pp. 267–276, 1996.
- [29] A. Acrivos, M. J. Shah, and E. E. Peterson, “Momentum and heat transfer in laminar boundary layer flow on non-newtonian fluids past external surfaces,” *AICHE Journal*, vol. 6, pp. 312–316, 1960.
- [30] W. R. Schowalter, “The application of boundary layer theory to power law pseudo plastic fluids: similar solutions,” *AICHE Journal*, vol. 6, 1960.
- [31] S. Y. Lee and W. F. Ames, “Similar solutions for non-newtonian fluids,” *AICHE Journal*, vol. 12, pp. 700–708, 1966.
- [32] H. I. Andersson, K. H. Bech, and B. S. Dandapat, “Magnetohydrodynamic flow of a power law fluid over a stretching sheet,” *International Journal of Non-Linear Mechanics*, vol. 72, no. 4, pp. 929–936, 1992.
- [33] C. Chein-Hsin, “Effects of magnetic field and suction/injection on convection heat transfer of non-newtonian power law fluids past a power law stretched sheet with surface heat flux,” *International Journal of Thermal Sciences*, vol. 47, pp. 954–961, 2008.
- [34] M. A. Seddeek, “Finite element method for the effect of viscous injection parameter on heat transfer for a power law non-newtonian fluid over a continuous stretched surface with thermal radiation,” *Computational Material Science*, vol. 37, pp. 642–627, 2006.

- [35] I. A. Hassanien, A. A. Abdullah, and R. S. R. Gorla, "Flow and heat transfer in a power law fluid over a non-isothermal stretching sheet," *Mathematical and Computer Modelling*, vol. 28, pp. 105–116, 1998.
- [36] R. Shyam, C. Sasmal, and R. P. Chhabra, "Natural convection heat transfer from two vertically aligned circular cylinders in power-law fluids," *International Journal of Heat and Mass Transfer*, vol. 64, pp. 1127–1152., 2013.
- [37] V. M. Soundalgekar, H. S. Takhar, and N. V. Vighnesam, "The combined free and forced convection flow past a semi infinite plate with variable surface temperature," *Nuclear Engineering Design*, vol. 10, p. 95, 1960.
- [38] M. A. Hossain and H. S. Takhar, "Radiation effect on mixed convection along a vertical plate with uniform surface temperature," *Heat Mass Transfer*, vol. 31, p. 243, 1996.
- [39] M. A. Hossain, M. A. Alim, and D. A. Rees, "The effect of radiation on free convection from a porous vertical plate," *International Journal of Heat Mass Transfer*, vol. 42, p. 181, 1999.
- [40] H. M. Duwairi and R. A. Damseh, "Mhd-buoyancy aiding and opposing flows with viscous dissipation effects from radiate vertical surfaces," *Canadian Journal of Chemical Engineering*, vol. 82, p. 613, 2004.
- [41] M. M. Rahman and T. Sultana, "Radiative heat transfer flow of micropolar fluid with variable heat flux in a porous medium," *Nonlinear Anal Model Control*, vol. 13, pp. 71–87, 2008.

- [42] M. S. Alam, M. M. Rahman, and M. A. Sattar, “Effects of variable suction and thermophoresis on steady mhd combined free-forced convective heat and mass transfer flow over a semi-infinite permeable inclined plate in the presence of thermal radiation,” *International Journal of Thermal Sciences*, vol. 47, p. 758, 2008.
- [43] M. S. Alam, M. M. Rahman, and M. A. Sattar, “On the effectiveness of viscous dissipation and joule heating on steady magnetohydrodynamic heat and mass transfer flow over an inclined radiate isothermal permeable surface in the presence of thermophoresis,” *Commun Nonlinear Sci Numer Simul*, vol. 14, p. 2132, 2009.
- [44] M. M. Rahman and K. M. Salahuddin, “Study of hydromagnetic heat and mass transfer flow over an inclined heated surface with variable viscosity and electric conductivity,” *Communication in Nonlinear Sciences of Numerical Simulation*, vol. 15, pp. 2073–2085, 2010.
- [45] K. Das, “Slip effects on heat and mass transfer in mhd micropolar fluid flow over an inclined plate with thermal radiation and chemical reaction,” *International Journal of Numerical Methods of Fluids*, vol. 70, pp. 96–113, 2012.
- [46] R. W. Fox and A. T. McDonald, *Introduction to Fluid Mechanics*. John WILEY and SONS, eighth ed., 2011.
- [47] J. Bear, *Dynamics of fluid in Porous media*. New York: Dover, 1972.
- [48] Symon and Keith, *Mechanics*. Addison Wesley, third ed., 1971.
- [49] R. B. Bird, R. C. Curtis, Armstrong, and O. Hassagee, *Dynamics of Polymeric Liquids*, vol. 2. New York: WILEY and Sons, second ed., 1987.

- [50] S. Asghar and C. M. K. K. Hanif, T. Hayat, “Mhd non-newtonian flow due to non-coaxial rotations of an accelerated disk and a fluid at infinity,” *Communication Non-linear Science Numerical Simulation*, vol. 12, pp. 465–485, 2007.
- [51] F. M. White, *Fluid Mechanics*. WCB McGraw-Hill, fourth ed.
- [52] F. P. Incropera and D. P. Dewitt, *Heat and Mass transfer*. India: Willey sons, fifth ed.